NUMERICAL SIMULATIONS OF ARGON-HYDROGEN RF THERMAL PLASMAS WITH ADDITIONAL GAS INJECTION

Takayuki Watanabe, Atsushi Kanzawa,
Takamasa Ishigaki*and Yusuke Moriyoshi*
Department of Chemical Engineering, Tokyo Institute of Technology,
O-okayama, Meguro-ku, Tokyo 152
* National Institute for Research in Inorganic Materials, Namiki, Tsukuba-shi, Ibaraki 305

ABSTRACT

Modeling of argon-hydrogen RF thermal plasmas with gas injection into the tailflame has been performed. Hydrogen injection results in the decreased temperature and axial velocity owing to hydrogen dissociation, while argon injection causes the increased temperature and axial velocity owing to the suppression of the radial outward flow of the plasma at the reaction chamber. The maximum concentration of hydrogen atom is obtained in the reaction chamber at a suitable flow rate of the injected hydrogen. The injection gas into the plasma tailflame has little effect on the plasma characteristics above the injection level.

1. INTRODUCTION

Radio-frequency induction thermal plasmas have a number of applications with chemical reactions: synthesis of ultrafine powders, deposition of thin films, and decomposition of chlorofluorocarbons. The distributions of the temperature, velocity and reactant or product concentration have been calculated because the understanding of these profiles is indispensable to development of novel plasma processing.

Some modeling approaches of RF thermal plasmas including chemical reactions have been proposed recently. Zhao et al. [1] presented modeling with reactions between $SiCl_4$ and H_2. McKelliget and El-Kaddah [2,3] also calculated plasma fields including the dissociation of $SiCl_4$. Girshick and Yu [4] reported the simulations of argon plasmas mixed with molecular gas, however they assumed equilibrium concerning the degree of the dissociation. The authors [5-7] presented modeling of argon plasmas mixed with molecular gas in consideration of its dissociation and recombination kinetics.

In the present work, numerical simulations of argon-hydrogen RF thermal plasmas with gas injection into the tailflame are performed. Modeling which is concerned with reactions caused by the gas injection in a reaction chamber is rather scarce. The determination of the gas injection effect on the plasma characteristics is important because the gas injection plays an important part in plasma processing such as the production of ultrafine Si_3N_4 powders [8]; the powders were produced from the reactant of $SiCl_4$ and NH_3, the latter being injected into the plasma tailflame. The purpose of the present work is to investigate the effect of gas injection into a plasma tailflame on the fields of velocity, temperature, and concentration in the reaction chamber as well as those in the plasma torch.

2. NUMERICAL FORMULATION

2.1 Basic Model and Assumptions

A model of the RF plasma torch and reaction chamber is shown in Fig. 1, and the operating conditions are summarized in Table 1. The model is also concerned with a steel injection tube along the torch axis. The model is applied to the plasma torch at a power level of 25 kW and induction frequency of 2 MHz. Argon is injected from the water-cooled steel tube (4 liters/min) and from inner slots (6 liters/min). The sheath gas injected with swirl from outer slots is the mixture of argon (30 liters/min) and hydrogen (3.5 liters/min). The conditions of the injection gas (argon or/and hydrogen) from circumference slots located below the plasma torch are varied to investigate its effect on the plasma characteristics.

The calculations are based on the following assumptions: (a) steady-state laminar flow; (b) axial symmetry; (c) optically thin; (d) negligible viscous dissipation; (e) negligible displacement current and flow-induced electric field; (f) local thermodynamic equilibrium for ionization (The dissociation and recombination rates of hydrogen are considered.)

2.2 Governing Equations

The fields of flow, temperature and concentration in the RF thermal plasma can be calculated by solving the two dimensional continuity, momentum (x,r, θ), energy and species conservation equations.

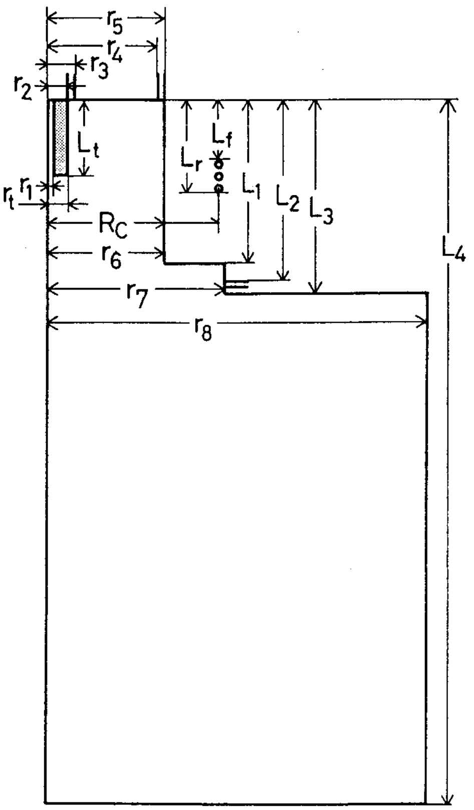

Fig.1 A schematic of the RF plasma torch and the reaction chamber.

Table 1 Parameters of the RF plasma torch.

Torch power	25 kW
Working frequency	2 MHz
Reactor pressure	400-760 torr
Coil radius (R_c)	34 mm
Coil turn number	3
Distance to frontal end of coil (L_f)	60 mm
Distance to rear end of coil (L_r)	90 mm
Wall thickness of quartz tube (w)	2 mm
Insertion length of steel tube (L_t)	80 mm
Torch length (L_1)	210 mm
Distance to circumference slot (L_2)	230 mm
Distance to reaction chamber (L_3)	240 mm
Total length of reactor (L_4)	740 mm
Flow rate of carrier gas (Ar)	4 liters/min
Flow rate of plasma gas (Ar)	6 liters/min
Flow rate of sheath gas (Ar)	30 liters/min
Flow rate of sheath gas (H_2)	3.5 liters/min
Inner radius of injection tube (r_1)	1.25 mm
Outer radius of injection tube (r_t)	3.75 mm
Inner radius of inner slot (r_2)	3.75 mm
Outer radius of inner slot (r_3)	5 mm
Inner radius of outer slot (r_4)	22.5 mm
Outer radius of outer slot (r_5)	23 mm
Inner radius of quartz tube (r_6)	23 mm
Inner radius of circumference slot (r_7)	35 mm
Inner radius of reaction chamber (r_8)	75 mm

Continuity : $\nabla \cdot (\rho \mathrm{u}) = 0$ (1)

Momentum : $\rho \mathrm{u} \cdot \nabla \mathrm{u} = -\nabla \mathrm{p} + \nabla \cdot \tau + \mathrm{J} \times \mathrm{B}$ (2)

Energy : $\rho \mathrm{u} \cdot \nabla h = \nabla \cdot (\frac{k}{c_p} \nabla h) - Q_r + \mathrm{J} \cdot \mathrm{E}$ (3)

Species : $\rho \mathrm{u} \cdot \nabla c = \nabla \cdot (\rho D \nabla c) + S$ (4)

where ρ is the density, u is the velocity, p is the pressure, τ is the viscous stress tensor, h is the enthalpy, k is the thermal conductivity, C_p is the specific heat at constant pressure, Q_r is the radiation loss per unit volume, c is the mass fraction, D is the diffusion coefficient, and S is the source term due to the dissociation or recombination of hydrogen. In these equations the conduction current (J), the magnetic flux density (B), and the electric field intensity (E) are obtained from Maxwell's equations.

A two-dimensional modeling approach on the electromagnetic (EM) fields has been proposed firstly based on the introduction of the vector potential [2,9-11]. The two-dimensional approach is necessary for the modeling including a metallic tube inserted into an RF plasma torch, which brings about an induced electric current in the tube. The EM fields in this study are analyzed on the basis of a two-dimensional modeling approach with the electric field intensity as the fundamental EM field variable[12]. Maxwell's equations are expressed in terms of the electric field intensity as follows:

$$\nabla^2 \mathrm{E} - \xi \sigma \frac{\partial \mathrm{E}}{\partial t} = 0 \quad (5)$$

where ξ is the magnetic permeability and σ is the electrical conductivity.

The recombination rate of hydrogen can be evaluated from the following rate constant [13]:

$$\mathrm{H} + \mathrm{H} + \mathrm{M} = \mathrm{H}_2 + \mathrm{M}$$
$$k = 1.0 \times 10^6 / T \quad (6)$$

where M is the third species. The dissociation rate is calculated using the equilibrium constant.

The thermodynamic and transport properties of an argon-hydrogen plasma were obtained from the same procedures described in Ref.7.

2.3 Calculation Procedures

The governing conservation equations were solved using SIMPLEC algorithm[14], which is a revision of SIMPLER algorithm [15]. The governing equations and the electric field intensity equation were solved using the control-volume technique. Grid points 54 by 43 were used for both x and r directions.

3. RESULTS AND DISCUSSION

3.1 Plasma Characteristics with Additional Gas Injection

The calculated streamlines, isotherms, and concentration contours of H and H_2 are shown in Fig. 2 (a)-(d), respectively. Computations were performed for argon-hydrogen plasmas at 500 torr with mixture gas injected into the tailflame; the flow rates of the injection gas are 10 liters/min for argon and 5 liters/min for hydrogen.

The flow field exhibits the characteristic recirculation above the coil region, caused by the Lorentz force. The weak recirculation is also formed below the coil region. The largest recirculation and the radial expansion of the plasma are observed in the reaction chamber located below the torch. The temperature field demonstrates that the gas injected from the steel injection tube or from the circumference slots is heated up rapidly.

The corresponding concentration profiles of hydrogen atom show that the concentration near the torch wall below the coil region is the highest because the hydrogen injected as the sheath gas is entrapped by the recirculation and is thermally decomposed into the atom. The high concentration region of hydrogen atom also exists on the centerline in the reaction chamber. The second high concentration region is due to the hydrogen injected into the

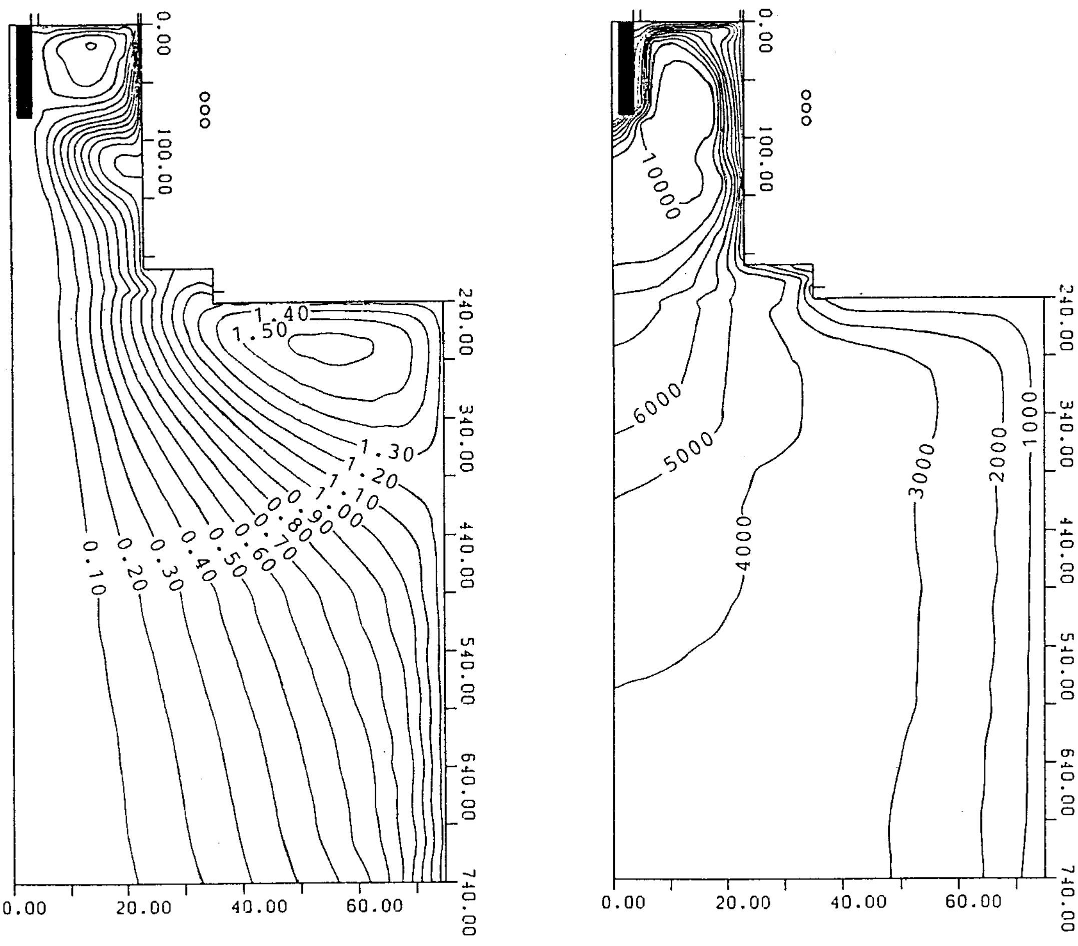

Fig.2 (a) Streamlines normalized by the mass flow rate in the plasma torch. (b) Isotherms.

plasma tailflame. This indicates that the sufficient mixing of the gas injected into the tailflame is achieved in the middle of the reaction chamber.

3.2 Effect of Additional Gas Injection

The effects of the gas injection into the plasma tailflame on the profiles of temperature, axial velocity, and hydrogen atom concentration along the centerline are represented in Figs. 3-5, respectively. Computational results for argon-hydrogen plasmas at 500 torr with additional hydrogen injection (5 - 15 liters/min) are compared to those with additional argon injection (5 liters/min) and to those without injection.

The temperature and the axial velocity below the injection level decrease when hydrogen is injected into the tailflame. The temperature decreases as the flow rate of the injected hydrogen increases. The decreased temperature results from hydrogen dissociation. However the temperature and the axial velocity below the injection level increase slightly when argon

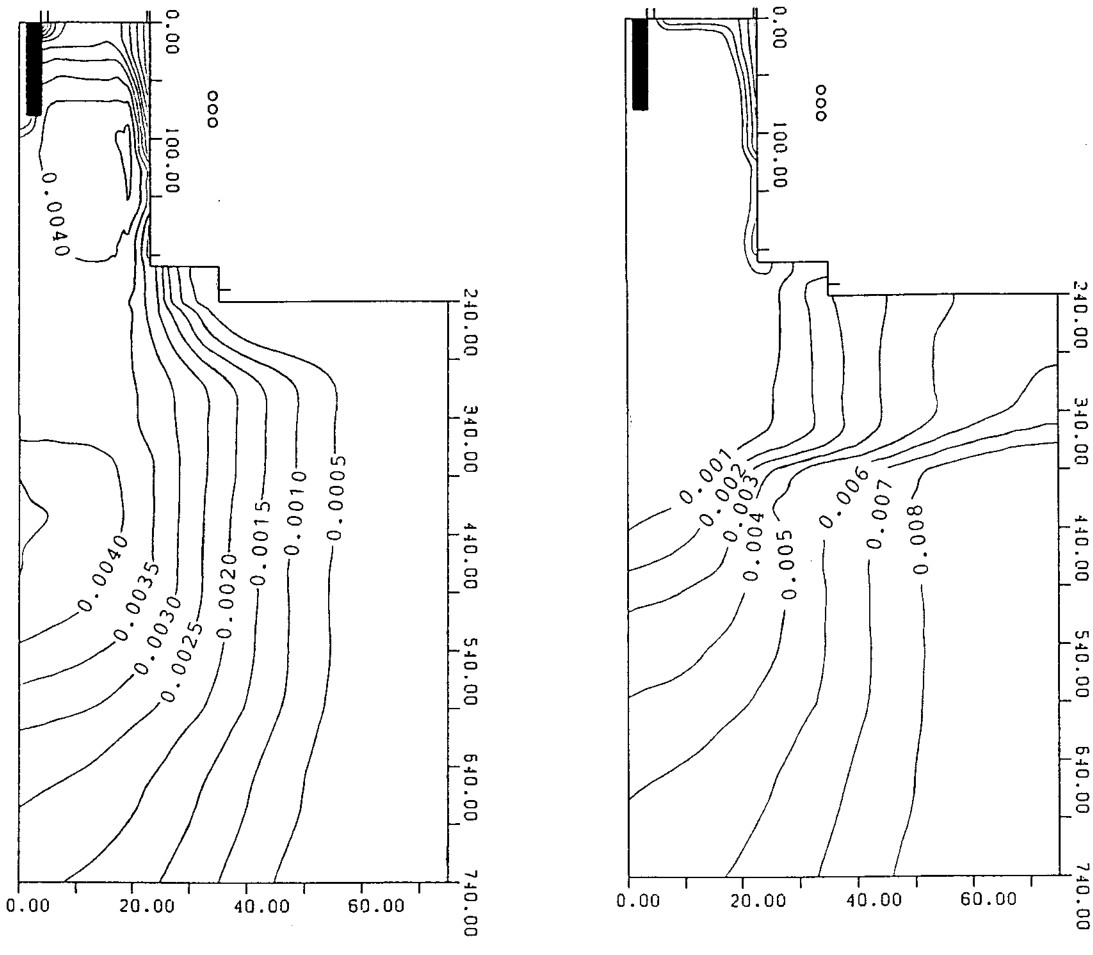

(c) Concentration contours of hydrogen atom.

(d) Concentration contours of hydrogen molecule.

is injected into the tailflame. The increased temperature and axial velocity are attributed to the suppression of the radial outward flow of the plasma at the reaction chamber. These plasmas with the hydrogen injection at various flow rates, with the argon injection, and without injection have almost the same profiles above the injection level, therefore the gas injection into the plasma tailflame has little effect on the plasma characteristics.

The profiles of hydrogen atom concentration show that the maximum can be obtained when hydrogen is injected at the flow rate of 10 liters/min. Moreover the concentration at the exit of the reaction chamber decreases with an increase in the flow rate of the injected hydrogen. Because the injected hydrogen with larger flow rate results in the decreased temperature as shown in Fig. 3, hence the decreased temperature causes lower degree of hydrogen dissociation.

3.3 Effect of Pressure Variation

The effects of the pressure variation on the characteristics of the plasma with additional gas injection are investigated by calculating the profiles of temperature and axial velocity as shown in Figs. 6 and 7, respectively. The pressure variation has attractive effect in ceramic powder treatment [16]. Computations were performed for argon-hydrogen plasmas with mixture gas injected into the tailflame; the flow rates of the gas are 10 liters/min for argon and 5 liters/min for hydrogen.

The axial velocity decreases with an increase in the pressure; the decrease in the velocity is due to the increase in the density. However the temperature along the centerline is little sensitive to the pressure, since the radiation loss from the plasma, which is proportional to the pressure, is not dominant near the centerline. These results are in qualitative agreement with the experimental observations; the length of the bright visible plasma, which roughly corresponds to the high temperature area over 9,000 K, is almost the same in the pressure range from 400 torr to 760 torr, while the radial extent of the bright plasma is slightly shrank

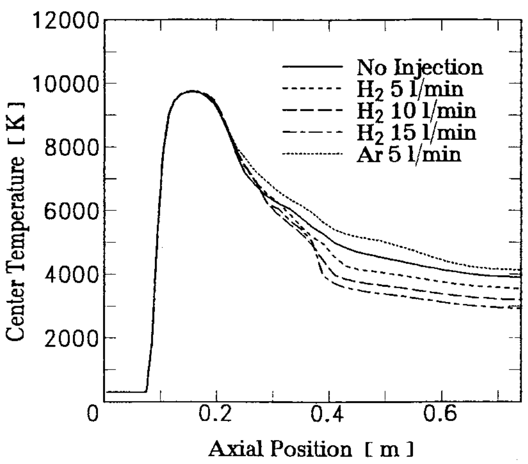

Fig.3 Effect of injection gas on temperature profiles along the centerline.

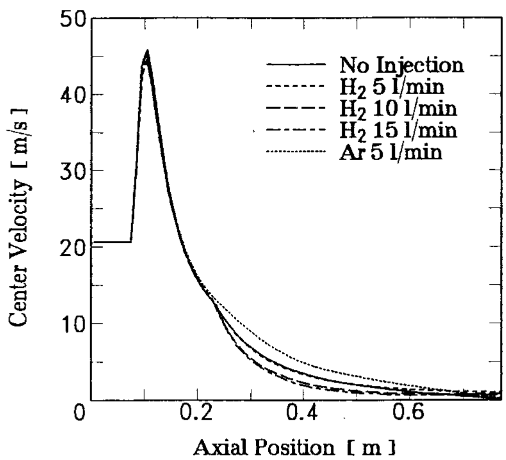

Fig.4 Effect of injection gas on axial velocity profiles along the centerline.

at higher pressure.

4. CONCLUSION

Numerical calculations were performed to simulate argon-hydrogen RF thermal plasmas with gas injection into the tailflame. The calculations gave the following results about the effects of the gas injection on the plasma characteristics.

The temperature and the axial velocity below the injection level were decreased by hydrogen injection owing to hydrogen dissociation, while these were increased slightly by argon injection owing to the suppression of the radial outward flow of the plasma at the reaction chamber. However the gas injection into the plasma tailflame had only little effect on the plasma characteristics above the injection level. The maximum concentration of hydrogen atom was obtained at a suitable flow rate of hydrogen injected into the tailflame.

The effects of the pressure variation were also investigated. The axial velocity decreased with an increase in the pressure, while the temperature along the centerline was almost the same at different pressures.

The present modeling is a powerful tool for the evaluation of additional gas

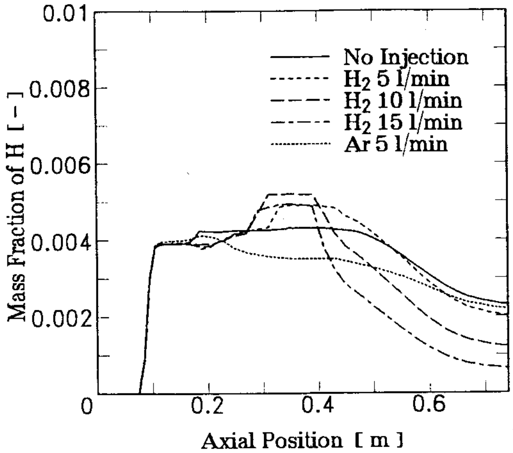

Fig.5 Effect of injection gas on mass fraction profiles of hydrogen atom along the centerline.

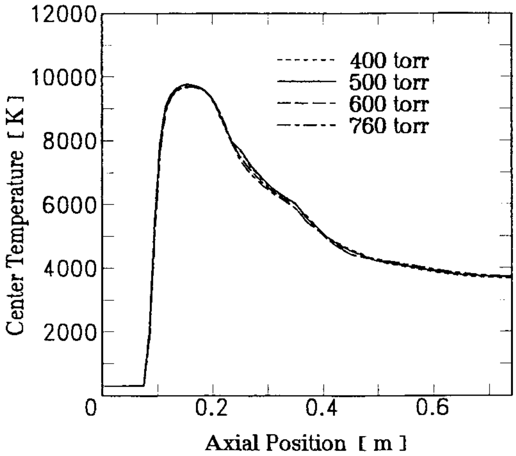

Fig.6 Effect of pressure variation on temperature profiles along the centerline.

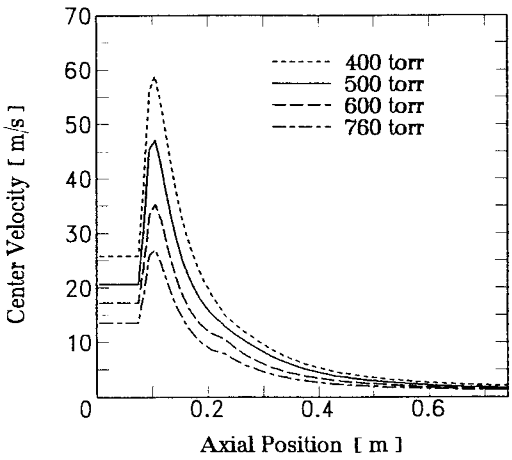

Fig.7 Effect of pressure variation on axial velocity profiles along the centerline.

injection into a plasma. The principle contribution of this work lies in the development of the approach including more complex chemical reactions.

REFERENCES

[1] G. Y. Zhao et al., Plasma Chem. Plasma Processing 10 (1990) 151.
[2] J. W. McKelliget and N. El-Kaddah, J. Appl. Phys. 64 (1988) 2948.
[3] J. W. McKelliget and N. El-Kaddah, Metall. Trans. 21B (1990) 589.
[4] S. L. Girshick and W. Yu, Plasma Chem. Plasma Processing 10 (1990) 515.
[5] T. Watanabe et al., J. Chem. Eng. Jpn. 24 (1991) 25.
[6] T. Watanabe et al., Proc. 10th Int. Symp. Plasma Chem. (1991) 1.1-31.
[7] T. Watanabe et al., J. High Temp. Soc. 17 (1991) 71.
[8] T. Yoshida et al., J. Appl. Phys. 54 (1983) 640.
[9] J. Mostaghimi et al., Plasma Chem. Plasma Processing 9 (1989) 25.
[10] X. Chen, J. Phys. D: Appl. Phys. 22 (1989) 361.
[11] X. Chen, Int. J. Heat Mass Transfer 33 (1990) 815.
[12] X. Chen and E. Pfender, Plasma Chem. and Plasma Processing 11 (1991) 103.
[13] Y. Mori et al., Formation Mechanisms and Controls of Pollutants in Combustion System, Japan Society of Mechanical Engineers (1980).
[14] J. P. Van Doormaal and G. D. Raithby, Num. Heat Transfer 7 (1984) 147.
[15] S. V. Patanker, Numerical Heat Transfer and Fluid Flow, McGraw-Hill, New York (1980).
[16] T. Ishigaki and M. I. Boulos, Ceramic Trans. 22 (1991) 139.